

Article

Application of Water Stable Isotopes for Hydrological Characterization of the Red River (Asia)

Nho Lan Nguyen ¹, Thu Nga Do ² and Anh Duc Trinh ^{3,*}

¹ Institute for Technology of Radioactive and Rare Earth Elements (ITRRE), Vietnam Atomic Energy Institute (VINATOM), 48 Lang Ha, Dong Da, Hanoi 11513, Vietnam; nguyennholan@gmail.com

² Faculty of Energy Technology, Electric Power University (EPU), 235 Hoang Quoc Viet, Cau Giay, Hanoi 11900, Vietnam; dothu_nga2005@yahoo.com

³ Nuclear Training Center (NTC), Vietnam Atomic Energy Institute (VINATOM), 140 Nguyen Tuan, Thanh Xuan, Hanoi 11416, Vietnam

* Correspondence: trinhahnduc@vinatom.gov.vn; Tel.: +84-906-006-808

Abstract: Fraction of young water (F_{yw}) and mean transit time (MTT, $\bar{\tau}$) calculated from water isotope profiles are valuable information for catchment hydrological assessment, especially in anthropogenically impacted region where natural conditions may not be decisive to catchment hydrology. The calculation of F_{yw} and MTT were performed on three subsets of $\delta^{18}\text{O}\text{-H}_2\text{O}$ data collected at the Hanoi meteo-hydrological station, Red River, in three periods; 2002–2005, 2015, and 2018–2019. The mean (min and max) values of $\delta^{18}\text{O}\text{-H}_2\text{O}$ in rainwater over the three periods are, respectively, -5.3‰ (-11.0 and -1.2‰), -5.4‰ (-10.7 and -1.4‰), and -4.5‰ (-13.9 and 1.7‰). The corresponding values in river water are -8.4‰ (-9.8 and -6.9‰), -8.5‰ (-9.1 and -7.7‰), and -8.4‰ (-9.5 and -7.2‰), respectively. The mean of F_{yw} calculated from the $\delta^{18}\text{O}\text{-H}_2\text{O}$ data for different periods is $22 \pm 9\%$, $10 \pm 5\%$, and $8 \pm 3\%$. Mean transit time is 4.69 ± 15.57 , 1.65 ± 1.53 , and 2.06 ± 1.87 years. The calculated F_{yw} (MTT) is negatively (positively) proportional to change in reservoir volume over the three periods, which is logical, since reservoirs tend to keep more water in the catchment and slower down water flow. The strong variation of F_{yw} and $\bar{\tau}$, two essential variables characterizing the catchment hydrology, represents an anthropogenic impact in the Red River system.

Keywords: regional water balance; fraction of young water; mean transit time; water stable isotopes; hydropower reservoirs



Citation: Nguyen, N.L.; Do, T.N.; Trinh, A.D. Application of Water Stable Isotopes for Hydrological Characterization of the Red River (Asia). *Water* **2021**, *13*, 2051. <https://doi.org/10.3390/w13152051>

Academic Editors: Tricia Stadnyk and David Widory

Received: 10 May 2021

Accepted: 24 July 2021

Published: 28 July 2021

Publisher's Note: MDPI stays neutral with regard to jurisdictional claims in published maps and institutional affiliations.



Copyright: © 2021 by the authors. Licensee MDPI, Basel, Switzerland. This article is an open access article distributed under the terms and conditions of the Creative Commons Attribution (CC BY) license (<https://creativecommons.org/licenses/by/4.0/>).

1. Introduction

The concentrations of oxygen and hydrogen isotopes in a water molecule undergo small changes during phase transitions. As a result, in different parts of the hydrologic cycle, water is naturally tagged with isotopic fingerprints, which vary according to the history of a particular body of water and its route through the hydrologic cycle. Since water isotopes are in water molecules, they are unique to trace the movements and storages of water in the hydrological cycle. Indeed, water stable isotopes ($\delta^{18}\text{O}$ or $\delta^2\text{H}$) are commonly used to investigate water storage in catchments [1–3]. Timescales of catchment storage are typically quantified by the mean transit time (MTT, $\bar{\tau}$), meaning the average time that elapses between parcels of water entering as precipitation and leaving again as streamflow [4]. The longer mean transit times imply greater damping of seasonal tracer cycles. Thus, the amplitudes of tracer cycles in precipitation and streamflow are commonly used to calculate catchment mean transit times. In addition to MTT, fraction of young water (F_{yw}), characterizing the storage capacity of a catchment, was recently proposed [5,6]. It is defined as the streamflow fraction that is roughly younger than three months after entering the catchment as meteoric water (e.g., precipitation). Estimation of F_{yw} is also done by comparing the amplitudes of sine waves, fitted to the seasonally varying isotope tracer signal in precipitation and streamflow. To date, this F_{yw} estimation method has only been

applied to theoretical datasets and smaller catchments in temperate areas [5–8]. It remains to be tested if Fyw can also be estimated for a complete river system (from headwater to estuary) where large reservoirs have been built to alter water course.

In developing and tropical countries, hydropower is a main energy source and large river systems such as the Red River, an interboundary river system, have been extensively exploited for power production. Extensive economic growth since the end of the 20th century in China and Vietnam has pushed a high demand for energy and water. Numerous large hydropower dams have been built in the Red River system during that period. A problem is that little information on hydropower dams (e.g., reservoir volume, operation plan) is exchanged among neighboring countries, causing difficulties for water resource development and management in countries located downstream of the river [9]. There is a need to revisit older dataset collected during the time of fewer hydropower projects and compare with contemporary data to see if and how hydropower development have impacted the river hydrology.

This paper represents the application of water isotopes for estimating of MTT and Fyw to the Red River, which has undergone intensive human alteration, especially hydropower production. The approach is considered simple, efficient, and particularly useful for interboundary river systems where comprehensive hydrological assessment is not always practicable. The broader aim is that the use of isotopic data for the calculation of principal hydrological characteristics will help inform regional stakeholders and policymakers in better water resource management practices. The time taken for water to travel from precipitation, through a catchment and to its outlet, is an important descriptor of the catchment functioning with broad implications for runoff generation, contaminant transport, and biogeochemical cycling [6].

2. Materials and Methods

2.1. Red River and Its Reservoirs Built Recently

The Red River stems from a mountainous area of Yunnan Province, China, at an elevation of 1776 m, flows southeasterly to Vietnam territory before emptying its water into Tonkin Bay. The total length of the main stream is 1149 km in which 510 km are in the Vietnam territory [10]. The total catchment area of the Red River is 169,020 km² in which 86,720 km² are in Vietnam. The Red River basin consists of 3 headwater mountainous sub-basins and 1 downstream delta area [11,12]. Three upstream-mountainous sub-basins, namely, Da, Lo, and Thao, merge their water together at Viet Tri, upstream of the delta area (Figure 1).

The region's climate is tropical monsoon with the rainy season between May and October. More than 80% of rainfall concentrates during this period. The mean discharge of the river at the river mouth is 2640 m³ s^{−1}, which highly fluctuates between dry and rainy seasons. Peaks of discharge usually occur in July–August [13].

Since 2007, in the Da sub-basin, China has put into operation about 11 hydroelectric projects with the total volume of about 2.5 billion m³ of water [9]. In the Vietnam territory, several large reservoirs such as Hoa Binh, Son, and Lai Chau have been built. These reservoirs were commissioned in the period of 1990–2016 (Table 1). In the Thao sub-basin, the Chinese side currently has about 29 reservoirs and dams including two large dams, Nanshan (commissioned around 2008) and Madushan (commissioned around 2011) [9,14] (Table 1). In Vietnam territory, no hydropower project has ever been established in this sub-basin. In the Lo sub-basin, the Chinese side has also built and operated about 8 hydropower reservoirs, of which 2 large reservoirs are Malutang (commissioned around 2018) and Baisheng (commissioned around 2010). In the Vietnam territory, a number of large reservoirs have been built, such as Thac Ba and Tuyen Quang. Thac Ba reservoir has been commissioned since 1972, and Tuyen Quang reservoir has been operated since 2010 [14] (Table 1).

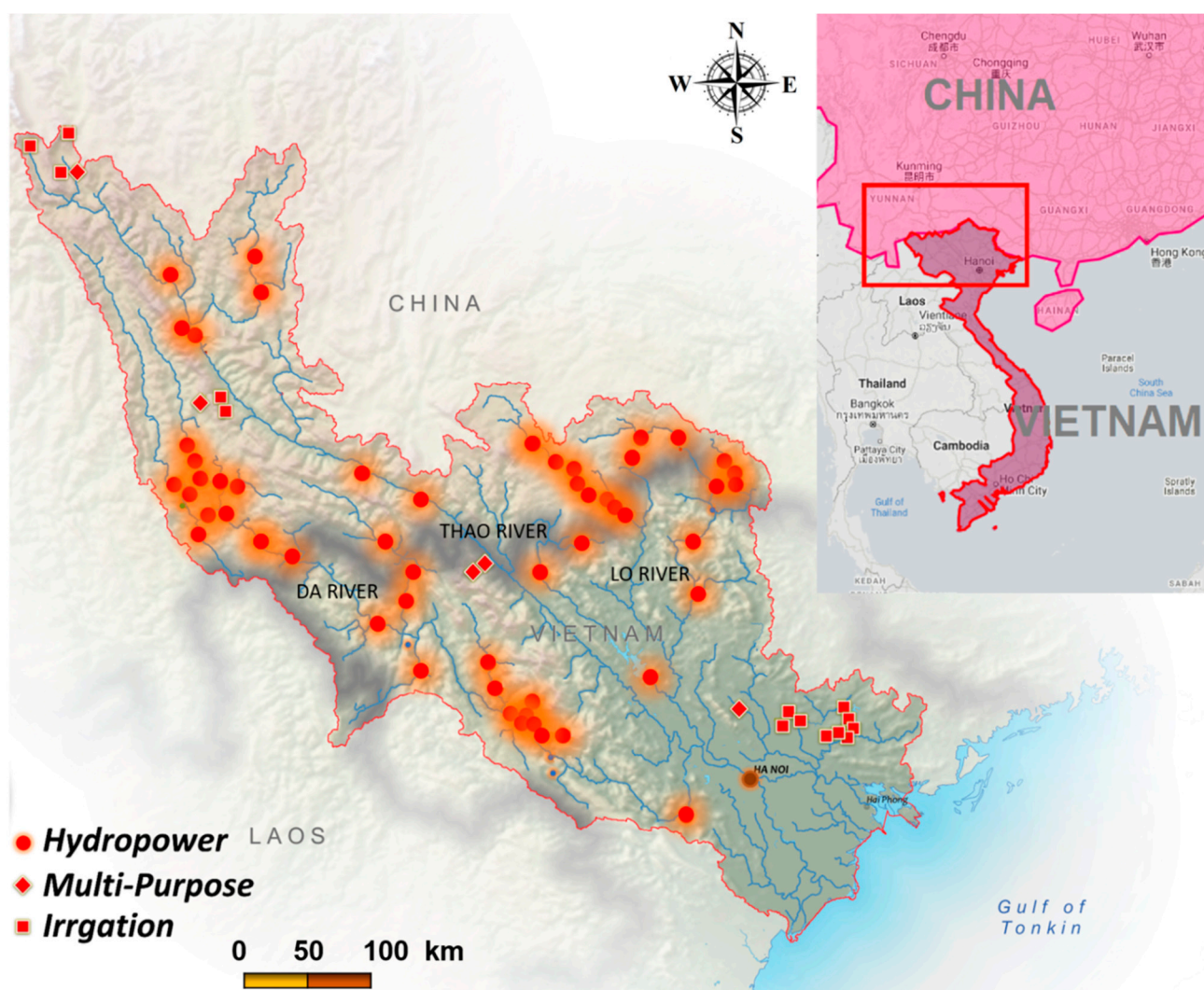


Figure 1. Dams in Red River basin and the Hanoi monitoring site.

2.2. Sampling Site and Analysis

River waters for water isotope analysis were collected monthly, usually in the middle of the month, at the Hanoi hydrological station (21°02′07.2″ N 105°51′58.1″ E). The monthly sampling protocol meets the standards set forth by the International Atomic Energy Agency (IAEA) [15]. Sampling was conducted in 3 periods; January 2003–December 2005, January 2015–December 2015, and January 2018–December 2019. Correspondingly, rainwater was also collected during the same periods.

The river water was collected by a bucket, filtrated through filter paper (8 µm pore size), and fully filled (avoiding bubbles) in 30 mL HDPE plastic bottles. They were then kept at 20 °C before being sent to the Isotope Hydrology Laboratory of IAEA, Vienna, Austria for analysis.

All samples were pipetted into 2 mL laser vials, and high-precision measurement using a Los Gatos Research liquid water isotope analyzer model 912-0032 (Los Gatos Research, CA, USA) was carried out. The method consisted of 9 injections per vial, excluding the first 4, with data processing procedures correcting for between-sample memory and instrumental drift, and normalization to the VSMOW-SLAP scale using LIMS for Lasers 2015 as fully described elsewhere [16,17]. A 2-point normalization used IAEA laboratory standards W-34 (low standard) and W-39 (high standard) to bracket the isotopic composition of the samples. IAEA laboratory standards were calibrated using VSMOW2 and SLAP2 primary reference materials with their assigned values of 0 ± 0.3 , $0 \pm 0.02\%$ and

$-427.5 \pm 0.3\text{‰}$, $-55.5 \pm 0.02\text{‰}$ for $\delta^2\text{H}$ and $\delta^{18}\text{O}$, respectively. The assigned values for the laboratory calibration standards W-39, W-34, and control W-31 were $+25.4 \pm 0.8\text{‰}$ and $+3.634 \pm 0.04\text{‰}$; $-189.5 \pm 0.9\text{‰}$ and $-24.778 \pm 0.02\text{‰}$; $-61.04 \pm 0.6\text{‰}$ and $-8.6 \pm 0.09\text{‰}$ for $\delta^2\text{H}$ and $\delta^{18}\text{O}$ relative to VSMOW, respectively. The control W-31 long-term (1-year running average) analytical reproducibility ($\pm\text{SD}$) was $\pm 0.11\text{‰}$ and $\pm 0.7\text{‰}$ for $\delta^{18}\text{O}$ and $\delta^2\text{H}$, respectively. It should be noted that in this paper, only $\delta^{18}\text{O}$ was used for the calculation of F_{yw} , as required by the method.

Table 1. Main reservoirs in the Red River system [9,14].

| Name | Country | Volume (million m ³) | Commision Year |
|------------|---------|----------------------------------|----------------|
| Thác Bà | Vietnam | 2940 | 1972 |
| Hòa Bình | Vietnam | 9862 | 1989 |
| Longma | China | 590 | 2007 |
| Jufudu | China | 174 | 2008 |
| Gelantan | China | 409 | 2008 |
| Tukahe | China | 88 | 2008 |
| Sinanjiang | China | 270 | 2008 |
| Malutang | China | 546 | 2018 |
| Sơn La | Vietnam | 9260 | 2010 |
| Shimenkan | China | 197 | 2010 |
| Madushan | China | 551 | 2011 |
| Lai Châu | Vietnam | 1215 | 2016 |
| Huổi Quảng | Vietnam | 184.2 | 2016 |
| Bản Chát | Vietnam | 162.7 | 2016 |
| Puxiqiao | China | 531 | 2016 |

Oxygen isotopic composition ($\delta^{18}\text{O}$, ‰) is defined as:

$$\delta^{18}\text{O} = \left[\frac{(^{18}\text{O}/^{16}\text{O})_{\text{Sample}}}{(^{18}\text{O}/^{16}\text{O})_{\text{VSMOW}}} - 1 \right] \times 1000\text{‰} \quad (1)$$

Whereas, $(^{18}\text{O}/^{16}\text{O})_{\text{Sample}}$ is a ratio of ^{18}O and ^{16}O abundances of sample and $(^{18}\text{O}/^{16}\text{O})_{\text{VSMOW}}$ is a ratio of ^{18}O and ^{16}O abundances of standard—Vienna Standard Mean Ocean Water.

2.3. Supplementary Data Acquisition

Monthly rainwater stable isotope data from Hanoi's GNIP stations were obtained from IAEA's NUCLEUS information resources. Meteo-hydrological data (rainfall and water discharge) collected daily at the Hanoi meteo-hydrological station (Figure 1) was acquired from the Vietnam National Hydro-Meteorological Station network. Water isotope data and meteo-hydrological data are provided in Table S1.

2.4. Estimation of MTT ($\bar{\tau}$) and F_{yw}

Both $\bar{\tau}$ and F_{yw} were calculated by fitting a sine wave to both the seasonal-varying precipitation and streamflow $\delta^{18}\text{O}$ isotope signals [6,7]. These are calculated, respectively, as:

$$C_P(t) = A_P \sin(2\pi ft - \varphi_P) + k_P \quad (2)$$

$$C_S(t) = A_S \sin(2\pi ft - \varphi_S) + k_S \quad (3)$$

where $C_p(t)$ is simulated precipitation and $C_s(t)$ is streamflow, $\delta^{18}\text{O}$ isotope values of time t (decimal years), A is the amplitude (‰), φ is the phase of the seasonal cycle (in radians, with 2π rad equaling 1 year), f is the frequency (yr^{-1}), and k (‰) is a constant describing the vertical offset of the isotope signal. After fitting these multiple regression equations, the Fyw can be calculated as:

$$Fyw = \frac{A_s}{A_p} \quad (4)$$

and $\bar{\tau}$ was calculated as:

$$\bar{\tau} = \alpha * \beta \quad (5)$$

where α and β are shape factor and scale factor, respectively. The shape factor (α) was implicitly expressed as:

$$\varphi_s - \varphi_p = \alpha \arctan\left(\sqrt{(A_s/A_p)^{-2/\alpha} - 1}\right) \quad (6)$$

and β was then calculated as:

$$\beta = \frac{1}{2\pi f} \sqrt{(A_s/A_p)^{-2/\alpha} - 1} \quad (7)$$

After α and β were determined, the mean transit time $\bar{\tau}$ was then calculated straightforwardly using Equation (5):

The OriginPro 2019 software providing the user-defined function/model was used for this regression analysis to obtain the coefficients A , φ , k_p , n , and m in Equations (2), (3), (6) and (7). The Levenberg–Marquardt algorithm was used to solve this generic curve-fitting problem.

Uncertainties in the calculated MTT and Fyw are expressed as standard errors (SEs) and are estimated using Gaussian error propagation (see Appendix A). Further description of the method can be found in [8].

Correlation analysis was used to assess the impact of forcing factors (rainfall, discharge, reservoir volume) on the MTT and Fyw over the monitoring years. The analysis was performed using OriginPro 2019 (9.65).

3. Results and Discussion

3.1. Meteo-Hydrological Seasonality

Rainfall data of three monitoring periods, 2003–2005, 2015, and 2018–2019, are shown in Figure 2a, which represents a clear rainy–dry seasonality with rainy peaks (about $400 \text{ mm month}^{-1}$) occurring in late summer: typical tropical monsoon climate [18,19]. The mean values of rainfall of three periods are, respectively, 148, 121, and $139 \text{ mm month}^{-1}$. Water discharge at the hydrological station of Hanoi is shown in Figure 2b. Mean discharges are, respectively, 2177, 1689, and $2058 \text{ m}^3 \text{ s}^{-1}$. It can be seen that discharge in 2015 and 2019 was lower than in other periods (about more than 20%). This can be explained by lower rainfall in 2015 and 2019 (approx. 20%) than in other periods. In terms of discharge, the dry season in 2015 (about 6 months) was longer than any of the other years (3–4 months) (Figure 2b).

3.2. Composition of Oxygen Isotopes— $\delta^{18}\text{O}$

The isotope composition of $\delta^{18}\text{O}$ of rainwater and river water in the study periods is shown in Figure 3. There is a clearly sinusoidal variability of rain and river water isotopic signal. The lowest value occurs during the rainy season and the highest value occurs during the dry season. This variability is agreed with a precedent study [20], which concluded that the equatorial–maritime air mass, well known for its amount effect (an inverse relationship between precipitation and the isotopic composition), dominates the precipitation regime in the region. Over the whole monitoring period, the mean (min and max) value of rainwater

$\delta^{18}\text{O}$ is -5.1‰ (-13.9 and 1.7‰). During the 2003–2005, the mean (min and max) values of rainwater and river water are -5.3‰ (-11 and -1.2‰) and 8.4‰ (-9.8 and -6.9‰), respectively. In 2015, the corresponding values are -5.4‰ (-10.7 and -1.4‰) and -8.5‰ (-9.1 and -7.7‰), respectively. During the 2018–2019, the values are -4.5‰ (-13.9 and 1.7‰) and -8.4‰ (-9.5 and -7.2‰), respectively.

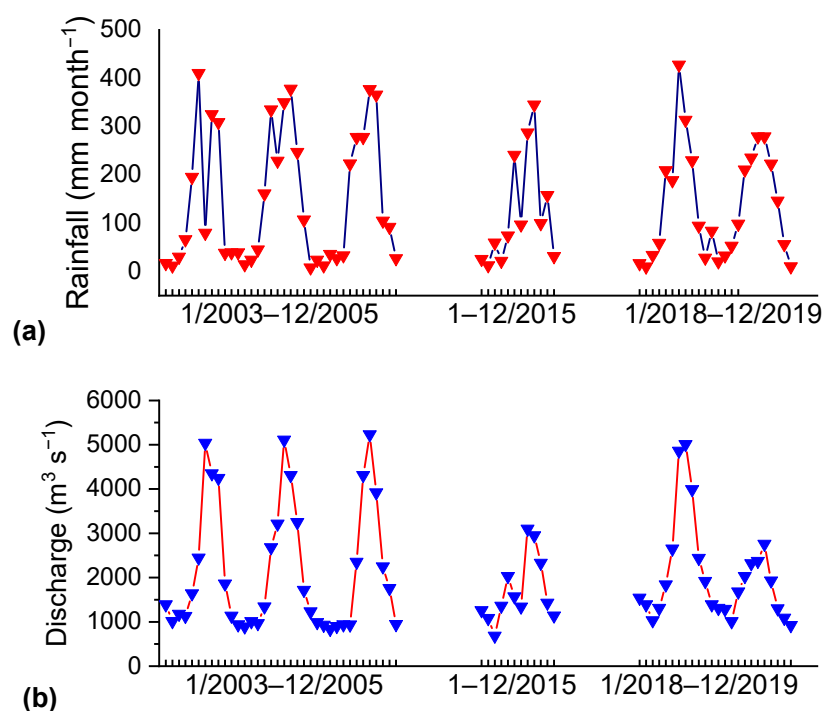


Figure 2. Monthly rainfall in Hanoi (a) and Red River's discharge at the Hanoi hydrological station (b).

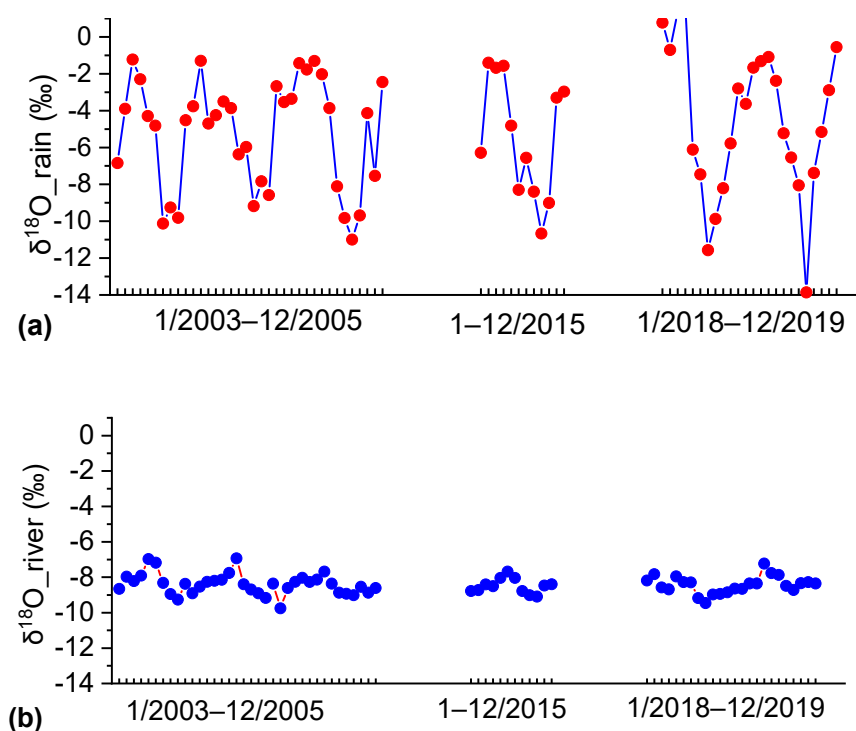


Figure 3. $\delta^{18}\text{O}$ in rainwater (a) and in river water (b).

3.3. Fraction of Young Water (F_{yw})

Minimum and maximum annual F_{yw} is, respectively, 7.96% and 31.76% (Figure 4). Over the three periods, F_{yw} decreases gradually, from 19.13% during the 2003–2005 period to 10.2% and 7.12% during the 2018–2019 period. The decreasing F_{yw} means that a fraction of older water components increases. There are various factors that can cause a change in F_{yw} , including external changes (e.g., rainfall) or changes inside watershed. The watershed changes may be natural processes of flows such as sedimentation, flow narrowing, or flow changes, but can also be caused by human impacts such as stream channeling, flow barring/dam building, or water saving. Among them, the interception and retention of water in hydropower reservoirs will increase the length of stay of the water, thereby increasing the age of the water and subsequently decreasing F_{yw} .

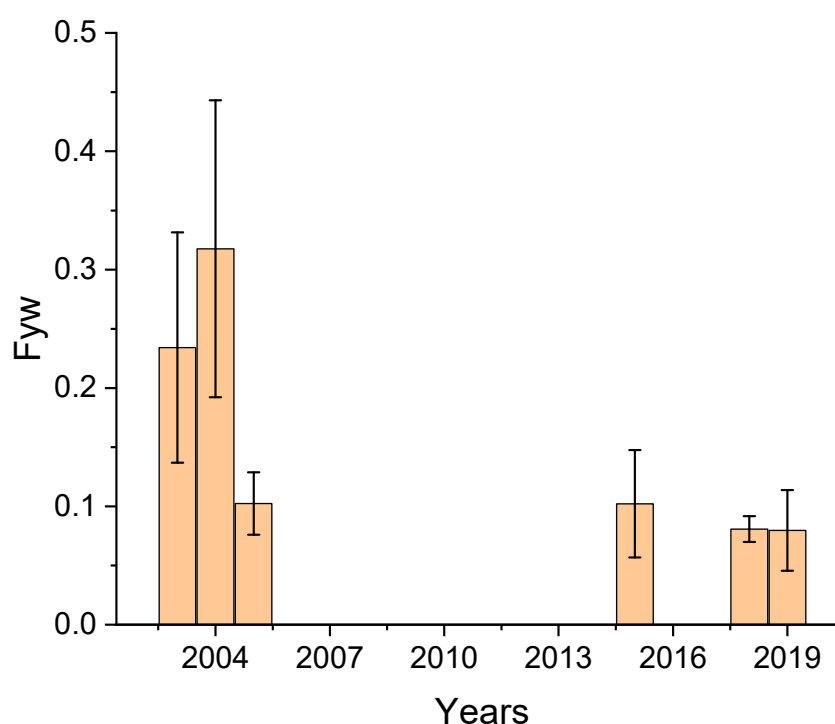


Figure 4. F_{yw} over the monitoring years.

3.4. Mean Transit Time ($\bar{\tau}$)

Mean transit time is calculated based on Equations (5)–(7), and the results show that mean transit time increases relatively over the monitoring years (Figure 5). Natural causes for an increase in MTT are, for example, an increase in vegetation coverage, reduction in precipitation, or natural extension of waterways [21–23]. This increase can also be explained by man-made constructions such as dams. The increasing number of hydropower dams in the Red River system recently could be a cause for the $\bar{\tau}$ increase, since hydropower dams hold back water to increase transit time. Peculiarly, MTT calculated for 2005 is high compared to the adjacent years. We are inclined to explain that the 2005 river water isotope profile, shown in Figure 3b, is less variable due to an unusual operation of hydropower dams to increase water storage during a long dry period. The precipitation data (Figure 2a) suggest that the 2004–2005 dry season was longer than usual. The monthly average precipitation during the dry season of 2005 is 23 mm, while the values of 2003 and 2004 are, respectively, 31 and 54 mm. To avoid falling to the non-operational water level, hydropower reservoirs in the Red River were being filled for a longer than usual time period. This critical operation is partly reflected by a low river discharge for six consecutive months (Figure 2b). Mean discharge during dry season of 2003, 2004, and 2005 at the Hanoi meteorological station is 1271, 1305, and 922 m³ s^{−1}, respectively. As a consequence, the river

water isotope signal at the Hanoi Site during dry period of 2005 was peculiarly lower than of other years—the longer mixing of different water sources in the reservoirs to average out the isotopic signal (Figure 3b). Thus, calculation on this less variable river water isotope profile resulted in a low Fyw (Figure 4) and a high MTT (Figure 5). This explanation is consistent with our assumption that hydropower reservoirs and their operation are critical to the Red River hydrology. Notably, MTT calculated for 2005 should be cautiously taken into account because of its high uncertainty (high SE) (Figure 5). In term of management practices, the success of using isotopes to identify the change in reservoir operation shows the potential of using isotopes to identify changes in regulation that may impact the river system ecohydrology.

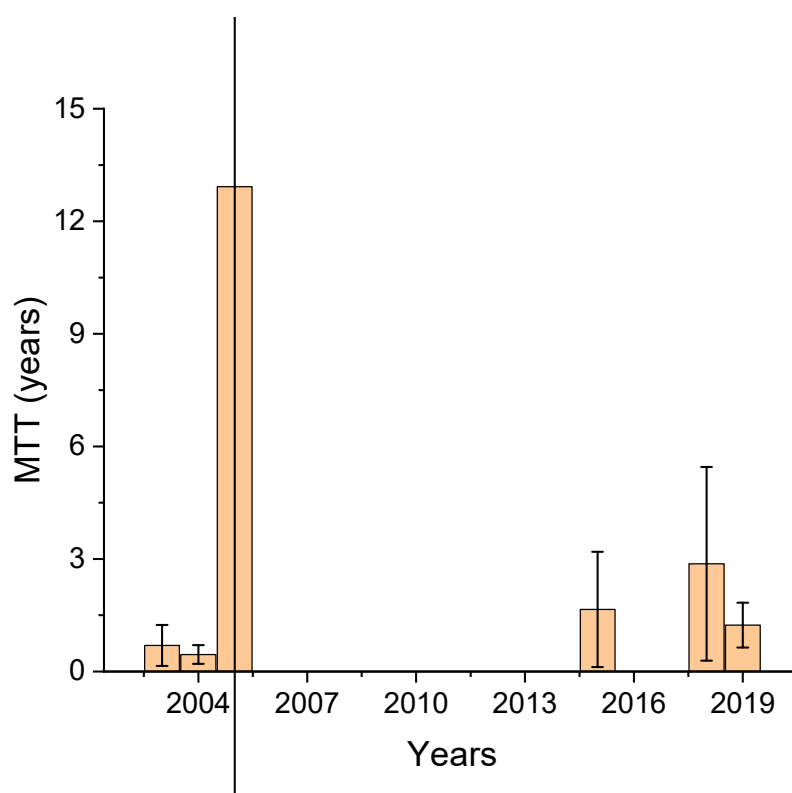
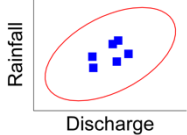
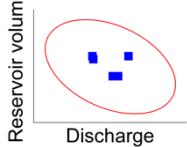
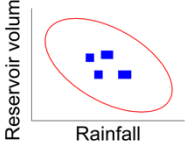

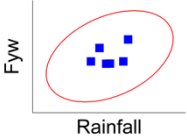
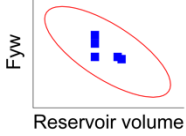
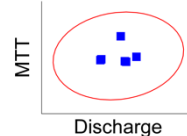
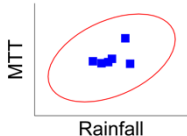
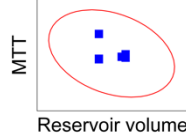
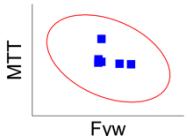


Figure 5. Mean transit time ($\bar{\tau}$).

3.5. Impact of Forcing Factors to the Red River Hydrology

Although our information about reservoir construction and commission in China is scarce, it is certain that the number of dams and the total reservoir volume on the Red River system has dramatically increased over the last 20 years. In the Vietnamese territory, until 2005, there were only two large reservoirs, the Hoa Binh and Thac Ba hydropower reservoirs, with a total storage capacity of about 12.8 billion m^3 . By 2015, the total volume of reservoirs increased to 24.5 billion m^3 and by 2018 was 27.0 billion m^3 (Table 1). Logically, in response to an increase in the number of reservoirs and the total reservoir volume is an increase in MTT and a decrease in Fyw . Thus, correlation analysis would help reveal a linkage between reservoir commission in Red River with MTT and Fyw (Table 2).

Table 2. Spearman correlation coefficients (p -values) between forcing factors (annual rainfall, annual discharge, reservoir volume) and hydrological variables (Fyw and MTT); data used for correlation calculation are in Appendix B.

| | Annual Discharge | Annual Rainfall | Reservoir Volume | Fyw | MTT |
|------------------|--|--|---|--|--------------|
| Annual discharge | 1 (–) | 0.49 (0.33) | –0.19 (0.73) | 0.43 (0.40) | –0.09 (0.87) |
| Annual rainfall |  | 1 (–) | –0.31 (0.55) | 0.37 (0.47) | –0.03 (0.96) |
| Reservoir volume |  |  | 1 (–) | –0.93 (0.01) | 0.28 (0.59) |
| Fyw |  |  |  | 1 (–) | –0.49 (0.33) |
| MTT |  |  |  |  | 1 (–) |

Bold: Significant correlation at p -value < 0.05. Ellipse: 95% confidence level.

Among forcing factors, we notice logical and insignificant tendencies; a positive correlation coefficient between annual rainfall and annual discharge (0.49) and negative coefficients between reservoir volume and annual discharge/annual rainfall (–0.19/–0.31). We interpret that in a year of high (low) rainfall, the river discharge would be high (low), producing a positive correlation between rainfall and runoff. On the other hand, an increase in reservoir volume would increase water storage in the catchments [24,25]. Hydrological processes related to the catchment storage variability such as infiltration, groundwater recharge, and evaporation are enhanced to reduce the surface water runoff. As a result, reservoir volume tends to correlate negatively with discharge and rainfall.

As expected, Fyw and accumulative volume of reservoirs are significantly negatively correlated with each other (at p -value < 0.05) (Table 2). To a lesser extent, the reservoir volume is positively and insignificantly correlated with MTT (Corr. Coef. = 0.28). Annually, there is a weak correlation between MTT and Fyw (Corr. Coef. = –0.49). Thus, correlation analysis suggests that hydrology in the Red River system (indicated by Fyw and $\bar{\tau}$) is severely altered by the commission of numerous hydropower reservoirs. In fact, the lower correlation between MTT and forcing factors than between Fyw and forcing factors is not a surprise. Kirchner [6] showed that the use of seasonal cycles in chemical or isotopic tracers to estimate MTT will typically be wrong by several hundred percent, when applied to catchments with realistic degrees of spatial heterogeneity such as the Red River Basin. This aggregation bias arises from the strong nonlinearity in the relationship between tracer cycle amplitude and mean travel time. Meanwhile, Fyw is accurately predicted by seasonal tracer cycles within a precision of a few percent, across the entire range of MTT from almost zero to almost infinity.

In theory, Fyw can be considered a catchment characteristic, analogous (but far from equivalent) to MTT. Mean transit time should be particularly useful as a catchment descriptor, because the MTT times the mean annual discharge yields the total catchment storage.

Fraction of young water, such as the amplitude of the seasonal tracer cycle, depends on the relative proportions of younger and older water, but is insensitive to how old the “older” water is. Meanwhile, MTT depends critically on the age of the older water, which cannot be reliably determined because it has almost no effect on the seasonal tracer cycle (or on more elaborate convolution analyses; see [7]). Because Fyw is indifferent to the age of the older water, it cannot be used to estimate residual storage.

What Fyw estimates, instead, is the fraction of water reaching the stream by relatively fast (less than 3 months) flowpaths. That, in turn, will depend on precipitation climatology. Concurrently, reservoirs are built to store rainwater (fast flow water). They are very much functioning with precipitation regime. Thus, Fyw would be explicitly useful in helping water resources managers assess the impact of reservoirs to the downstream flow regime.

Apart from the reservoir volume– Fyw /MTT relationship, a positive and insignificant correlation between Fyw and annual discharge (Corr. Coef. = 0.43) and annual rainfall (Corr. Coef. = 0.37) is found. A possible explanation for this positive correlation is that at intensified rain events, new fast flow paths are formed in sloping lands to increase Fyw in river flow [8]. From the management perspective, this positive discharge/rainfall– Fyw relationship is not encouraging, since fast flow paths are related to soil erosion, landslides, and flash floods in headwater catchments. Indeed, such hazards have been widely reported in the media recently [20,26–28].

Besides the catchment heterogeneity issue, a weak correlation between MTT and forcing factors (Table 2) could also be due to the sparseness and uncertainty of our dataset. As discussed in the previous sub-section, the low variability of isotope profile due to unusual hydropower dam operation results in an MTT of a peculiarly high uncertainty (high SE) for 2005 (Figure 5). Statistically, including the 2005 data into regression analysis is not significant. If the 2005 data were excluded, the correlation coefficient (p-value) between MTT and discharge, rainfall, and reservoir volume would, respectively, be 0.10 (0.87), -0.30 (0.62), and 0.79 (0.11), higher than when these 2005 data were included and close to the Fyw -forcing factor coefficients (Table 2). Importantly, the new calculated trends are logical; MTT would increase with the reservoir volume and decrease with the annual rainfall. This observation implies that analysis of a sparse but accurate dataset still provides reliable and meaningful results. The results here also reinforce the operational value of using isotopes as “early indicators” of operational change and subsequent hydrologic functions of a catchment.

All the same, the correlation analysis suggests that reservoirs always play a major role controlling these hydrological variables (high Corr. Coef.). To a lesser degree, rainfall is a formidable factor changing Fyw and MTT. In contrast, discharge in the Red River is well controlled by hydropower dams and so does not pose a particular relationship with hydrological variables (low Corr. Coef.). Depending on the extreme events occurring during the year or inter-annually, the dams will control the flow regime and then modify MTT and Fyw . Above all, humans appear to be the biggest forcing factor regulating the Red River hydrology.

4. Conclusions

Results from this study suggest that mean transit time increases and the Fyw decreases due to the impact of water storage from dams in the upstream area in the Red River system.

Together with MTT, Fyw is a highly reliable variable applied to hydrological assessment in heterogeneous, anthropogenic impacted basins such as the Red River and Mekong River Systems. The approach is simple and straightforward, needed only water stable isotope data, and can be used by student level practitioners.

This study shows a versatility of isotopic tracers to assess water regime change/hydrology. Water stable isotopes as compared to other artificial tracers are unique of their own and should be highly appreciated in water resources research programs. Regrettably, not many people including stakeholders and water managers in the region understand the comprehensive application of water isotopes for water resources assessment and monitoring.

High uncertainty of some calculated results implies that further investigation is needed to enrich the currently sparse dataset. The investigation should be conducted at other sites to downscale the Red River basin into smaller domains with and without severely anthropogenic impacts. Data obtained from smaller domains characterized with different impacts would help to make a firm conclusion on the role of hydropower reservoirs and other forcing factors to the river hydrology.

It is necessary to have cooperation and strengthening of information sharing between Vietnam and China for hydrological research of the Red River basin in order to obtain more accurate and meaningful results in water resource management and exploitation.

Globally, the number of dam constructions has increased dramatically over the past six decades and is forecast to continue to rise, particularly in less industrialized regions and that identifying development pathways that can deliver the benefits of new infrastructure while also maintaining healthy and productive river systems is a great challenge that requires understanding the multifaceted impacts of dams at a range of scales [29]. In this context, the isotopically based approach can be used as a simple and reliable tool to improve predictions of how dam construction will affect ecohydrology, ecosystem functioning, and fluvial geomorphology worldwide, helping to frame a global strategy to achieve sustainable dam development.

Supplementary Materials: The following are available online at <https://www.mdpi.com/article/10.3390/w13152051/s1>, Rainfall, river discharge and water stable isotope data at Ha Noi Site.

Author Contributions: Conceptualization, A.D.T. and T.N.D.; methodology, A.D.T.; software, N.L.N.; validation, A.D.T. and N.L.N.; formal analysis, N.L.N.; investigation, N.L.N. and A.D.T.; resources, A.D.T.; data curation, N.L.N.; writing—original draft preparation, N.L.N.; writing—review and editing, A.D.T. and T.N.D.; visualization, A.D.T. and N.L.N.; supervision, A.D.T.; project administration, A.D.T.; funding acquisition, A.D.T. All authors have read and agreed to the published version of the manuscript.

Funding: This research was funded by the Ministry of Science and Technology of Vietnam (MOST) and Austrian agency for international mobility and cooperation in education, science, and research (OeAD)—No. 05-2020 “Ứng dụng kỹ thuật đồng vị trong nghiên cứu quá trình thủy văn trong sông Hồng và các chi lưu”.

Institutional Review Board Statement: Not applicable.

Informed Consent Statement: Not applicable.

Data Availability Statement: The data presented in this study are available in supplementary material.

Acknowledgments: Special thanks are sent to Leonard I Wassenaar, IAEA, for his precious assistance in water stable isotope analysis. We also appreciate the financial support for water sampling and monitoring from LMI-LUSES (luses.ird.fr) and NTC, VINATOM (De tài cap co so 2021).

Conflicts of Interest: The authors declare no conflict of interest. The funders had no role in the design of the study; in the collection, analyses, or interpretation of data; in the writing of the manuscript, or in the decision to publish the results.

Appendix A

Formulation of SE Calculation for F_{yw} and MTT ($\bar{\tau}$)

- Calculation of σ_α

Starting from:

$$\varphi_S - \varphi_P = \alpha \arctan \left(\sqrt{(A_S/A_P)^{-2/\alpha} - 1} \right) \quad (A1)$$

To name: $\varphi = \varphi_S - \varphi_P$ and $A = A_S/A_P$

We have,

$$\varphi = \alpha \arctan\left(\sqrt{A^{-2/\alpha} - 1}\right) \quad (\text{A2})$$

$$\sigma_{\varphi}^2 = \left(\frac{\partial \varphi}{\partial \alpha}\right)^2 * \sigma_{\alpha}^2 + \left(\frac{\partial \varphi}{\partial A}\right)^2 * \sigma_A^2 \quad (\text{A3})$$

Thus, σ_{φ} can be calculated by the expression:

$$\sigma_{\varphi}^2 = \left(\frac{A^{-\frac{2}{\alpha}} * \ln(A^2) + \alpha * \arctan\left(A^{-\frac{2}{\alpha}} - 1\right) + \alpha * \left(A^{-\frac{2}{\alpha}} - 1\right)^2 * \arctan\left(A^{-\frac{2}{\alpha}} - 1\right)}{\alpha * \left(A^{-\frac{2}{\alpha}} - 1\right)^2 + \alpha} \right)^2 * \sigma_{\alpha}^2 + \left(\frac{-2 * A^{-\frac{2}{\alpha} - 1}}{1 + \left(A^{-\frac{2}{\alpha}} - 1\right)^2} \right)^2 * \sigma_A^2 \quad (\text{A4})$$

$$\begin{aligned} & \sigma_{\alpha}^2 \\ &= \left(\sigma_{\varphi}^2 - \left(\frac{-2 * A^{-\frac{2}{\alpha} - 1}}{1 + \left(A^{-\frac{2}{\alpha}} - 1\right)^2} \right)^2 * \sigma_A^2 \right) \\ & * \left(\frac{\alpha * \left(A^{-\frac{2}{\alpha}} - 1\right)^2 + \alpha}{A^{-\frac{2}{\alpha}} * \ln(A^2) + \alpha * \arctan\left(A^{-\frac{2}{\alpha}} - 1\right) + \alpha * \left(A^{-\frac{2}{\alpha}} - 1\right)^2 * \arctan\left(A^{-\frac{2}{\alpha}} - 1\right)} \right)^2 \end{aligned} \quad (\text{A5})$$

The calculation of σ_{α}^2 and σ_A were performed with Microsoft excel.

- Calculation of σ_{β}

$$\beta = \frac{1}{2\pi f} \sqrt{(A_S / A_P)^{-2/\alpha} - 1} \quad (\text{A6})$$

$$\beta = \frac{1}{2\pi f} \sqrt{A^{-2/\alpha} - 1} \quad (\text{A7})$$

$$\sigma_{\beta}^2 = \left(\frac{A^{-\frac{2}{\alpha}} * \ln A}{2 * PI * \alpha^2 * \left(A^{-\frac{2}{\alpha}} - 1\right)^{\frac{1}{2}}} \right)^2 * \sigma_{\alpha}^2 + \left(-\frac{A^{-\frac{2}{\alpha} - 1}}{2 * PI * \alpha * \left(A^{-\frac{2}{\alpha}} - 1\right)^{\frac{1}{2}}} \right)^2 * \sigma_A^2 \quad (\text{A8})$$

The calculation of σ_{β}^2 and σ_{β} were performed with Microsoft excel.

- Calculation of $\sigma_{\bar{\tau}}$

$$\sigma_{\bar{\tau}} = \bar{\tau} * \sqrt{\left(\frac{\sigma_{\alpha}}{\alpha}\right)^2 + \left(\frac{\sigma_{\beta}}{\beta}\right)^2} \quad (\text{A9})$$

- Calculation of $\sigma_{F_{yw}}$

$$\sigma_{F_{yw}} = F_{yw} * \sqrt{\left(\frac{\sigma_{As}}{As}\right)^2 + \left(\frac{\sigma_{Ap}}{Ap}\right)^2} \quad (\text{A10})$$

Appendix B

Data Used for Correlation Calculation

Table A1. Annual precipitation, monthly mean discharge, reservoir volume, F_{yw} , and MTT over the monitoring years.

| Year | Discharge ($\text{m}^3 \text{ s}^{-1}$) | Rainfall (mm month^{-1}) | Reservoir Volume (mill m^3) | F_{yw} | MTT (years) |
|------|--|--|---|----------|----------------|
| 2003 | 2197 | 130 | 12,802 | 0.23 | 0.70 |
| 2004 | 2226 | 160 | 12,802 | 0.32 | 0.45 |
| 2005 | 2109 | 155 | 12,802 | 0.10 | 12.93 |
| 2015 | 1689 | 121 | 24,887 | 0.10 | 1.65 |
| 2018 | 2448 | 141 | 26,980 | 0.08 | 2.87 |
| 2019 | 1668 | 137 | 26,980 | 0.08 | 1.24 |

References

- Rodriguez, N.B.; Pfister, L.; Zehe, E.; Klaus, J. Testing the truncation of travel times with StorAge Selection functions using deuterium and tritium as tracers. *Hydrol. Earth Syst. Sci. Discuss.* **2019**, 1–37. [\[CrossRef\]](#)
- Rodriguez, N.B.; Pfister, L.; Zehe, E.; Klaus, J. A comparison of catchment travel times and storage deduced from deuterium and tritium tracers using StorAge Selection functions. *Hydrol. Earth Syst. Sci.* **2021**, 25, 401–428. [\[CrossRef\]](#)
- Zhou, J.; Liu, G.; Meng, Y.; Xia, C.; Chen, K.; Chen, Y. Using stable isotopes as tracer to investigate hydrological condition and estimate water residence time in a plain region, Chengdu, China. *Sci. Rep.* **2021**, 11, 2812. [\[CrossRef\]](#)
- Bansah, S.; Andam-Akorful, S.A.; Quaye-Ballard, J.; Wilson, M.C.; Gidigas, S.S.; Anornu, G.K. An Evaluation of Catchment Transit Time Model Parameters: A Comparative Study between Two Stable Isotopes of Water. *Geosciences* **2019**, 9, 318. [\[CrossRef\]](#)
- Stockinger, M.P.; Bogen, H.R.; Lücke, A.; Stump, C.; Vereecken, H. Time variability and uncertainty in the fraction of young water in a small headwater catchment. *Hydrol. Earth Syst. Sci.* **2019**, 23, 4333–4347. [\[CrossRef\]](#)
- Kirchner, J.W. Aggregation in environmental systems—Part 1: Seasonal tracer cycles quantify young water fractions, but not mean transit times, in spatially heterogeneous catchments. *Hydrol. Earth Syst. Sci.* **2016**, 20, 279–297. [\[CrossRef\]](#)
- Kirchner, J.W. Aggregation in environmental systems—Part 2: Catchment mean transit times and young water fractions under hydrologic nonstationarity. *Hydrol. Earth Syst. Sci.* **2016**, 20, 299–328. [\[CrossRef\]](#)
- Freyberg, J.V.; Allen, S.T.; Seeger, S.; Weiler, M.; Kirchner, J.W. Sensitivity of young water fractions to hydro-climatic forcing and landscape properties across 22 Swiss catchments. *Hydrol. Earth Syst. Sci.* **2018**, 22, 3841–3861. [\[CrossRef\]](#)
- Ha, V.K.; Vu, T.M.T. Research the effect of upstream reservoirs on China to flow regime of Da River and Thao River. *J. Water Resour. Environ. Eng.* **2012**, 334, 199–214.
- Strady, E.; Dang, T.H.; Dao, T.D.; Dinh, H.N.; Do, T.T.D.; Duong, T.N.; Chu, V.H. Baseline assessment of microplastic concentrations in marine and freshwater environments of a developing Southeast Asian country, Viet Nam. *Mar. Pollut. Bull.* **2021**, 162, 111870. [\[CrossRef\]](#) [\[PubMed\]](#)
- Le, T.P.Q.; Billen, G.; Garnier, J.; Théry, S.; Fézard, C.; Chau, V.M. Nutrient (N, P) budgets for the Red River basin (Vietnam and China). *Glob. Biogeochem. Cycles* **2005**, 19, 19.
- Luu, T.N.M.; Garnier, J.; Billen, G.; Orange, D.; Némery, J.; Le, T.P.Q.; Tran, H.T.; Le, L.A. Hydrological regime and water budget of the Red River Delta (Northern Vietnam). *J. Asian Earth Sci.* **2010**, 37, 219–228. [\[CrossRef\]](#)
- Le, N.D.; Le, T.P.Q.; Hoang, T.T.H.; Phung, T.X.B.; Pham, T.M.H. Heavy metals in suspended solids in the Red river system at Chuong Duong bridge (Hanoi) (in Vietnamese). *J. Sci. Technol.* **2020**, 56, 114–118.
- Phung, T.X.B. *Study on the Effects of Upstream Reservoirs on the Conveyance of Suspended Sediment and the Binding Substances (C, N, P, and Si) in the Water in the Downstream Area of the River*; Ministry of Industry and Trade: Hanoi, Vietnam, 2019.
- IAEA. Water Isotope System for Data Analysis, Visualization and Electronic Retrieval. 2016. Available online: <https://nucleus.iaea.org/wiser/> (accessed on 30 April 2016).
- Wassenaar, L.; Coplen, I.; Aggarwal, P.K. Approaches for Achieving Long-Term Accuracy and Precision of $\delta^{18}\text{O}$ and $\delta^2\text{H}$ for Waters Analyzed using Laser Absorption Spectrometers. *Environ. Sci. Technol.* **2014**, 48, 1123–1131. [\[CrossRef\]](#)
- Coplen, T.B.; Wassenaar, L.I. LIMS for Lasers 2015 for achieving long-term accuracy and precision of $\delta^2\text{H}$, $\delta^{17}\text{O}$, and $\delta^{18}\text{O}$ of waters using laser absorption spectrometry. *Rapid Commun. Mass Spectrom.* **2015**, 29, 2122–2130. [\[CrossRef\]](#) [\[PubMed\]](#)
- Vu, V.H.; Merkel, B.J. Estimating groundwater recharge for Hanoi, Vietnam. *Sci. Total. Environ.* **2019**, 651, 1047–1057.
- Dang, T.A.T.; Wraith, D.; Bambrick, H.; Dung, N.; Truc, T.T.; Tong, S.; Dunne, M.P. Short-term effects of temperature on hospital admissions for acute myocardial infarction: A comparison between two neighboring climate zones in Vietnam. *Environ. Res.* **2019**, 175, 167–177. [\[CrossRef\]](#)
- Trinh, A.D.; Luu, T.N.M.; Le, T.P.Q. Use of stable isotopes to understand run-off generation processes in the Red River Delta. *Hydrol. Process.* **2017**, 31, 3827–3843. [\[CrossRef\]](#)
- Ma, W.; Yamanaka, T. Factors controlling inter-catchment variation of mean transit time with consideration of temporal variability. *J. Hydrol.* **2016**, 534, 193–204. [\[CrossRef\]](#)

-
22. Cartwright, I.; Morgenstern, U. Using tritium to document the mean transit time and sources of water contributing to a chain-of-ponds river system: Implications for resource protection. *Appl. Geochem.* **2016**, *75*, 9–19. [[CrossRef](#)]
 23. Jódar, J.; Custodio, E.; Lambán, L.J.; Martos-Rosillo, S.; Herrera-Lameli, C.; Sapriza-Azuri, G. Vertical variation in the amplitude of the seasonal isotopic content of rainfall as a tool to jointly estimate the groundwater recharge zone and transit times in the Ordesa and Monte Perdido National Park aquifer system, north-eastern Spain. *Sci. Total. Environ.* **2016**, *573*, 505–517. [[CrossRef](#)] [[PubMed](#)]
 24. Muhammad, A.; Evenson, G.R.; Unduche, F.; Stadnyk, T.A. Climate Change Impacts on Reservoir Inflow in the Prairie Pothole Region: A Watershed Model Analysis. *Water* **2020**, *12*, 271. [[CrossRef](#)]
 25. Muhammad, A.; Evenson, G.R.; Stadnyk, T.A.; Boluwade, A.; Jha, S.K.C.P. Assessing the Importance of Potholes in the Canadian Prairie Region under Future Climate Change Scenarios. *Water* **2018**, *10*, 1657. [[CrossRef](#)]
 26. Dang, N.M.; Babel, M.S.; Luong, H.T. Evaluation of food risk parameters in the day river flood diversion area, Red River delta, Vietnam. *Nat. Hazards* **2011**, *56*, 169–194. [[CrossRef](#)]
 27. Nguyen, D.G. The impact of the upstream reservoir system on the variations of hydrological and hydraulic regimes and riverbeds on the downstream side. *J. Water Resour. Sci. Technol.* **2016**, *32*, 29–36.
 28. McElwee, P.; Nghiem, T.; Le, H.; Vu, H. Flood vulnerability among rural households in the Red River Delta of Vietnam: Implications for future climate change risk and adaptation. *Nat. Hazards* **2016**, *86*, 465–492. [[CrossRef](#)]
 29. Grill, G.; Lehner, B.; Lumsdon, A.E.; MacDonald, G.K.; Zarfl, C.; Liermann, C.R. An index-based framework for assessing patterns and trends in river fragmentation and flow regulation by global dams at multiple scales. *Environ. Res. Lett.* **2015**, *10*, 015001. [[CrossRef](#)]